Cure Kinetics and Thermomechanical Properties of Thermally Stable Photopolymerized Dimethacrylates

Wayne D. Cook,[1] John S. Forsythe,[1] Nova Irawati,[2] Timothy F. Scott,[1] Wilson Z. Xia[1]

[1]*School of Physics and Materials Engineering, P.O. Box 69M, Monash University, Victoria, Australia, 3800*
[2]*CRC for Polymers, 32 Business Park Drive, Notting Hill, Victoria, Australia, 3168*

Received 2 December 2002; accepted 6 February 2003

ABSTRACT: A range of dimethacrylates with varying backbone flexibility were partially photocured to various conversions using *p*-xylylene bis-(*N*,*N*-diethyldithiocarbamate) as a photoiniferter and their glass transition region investigated by dynamic mechanical thermal analysis. For isothermally cured samples, the final degree of conversion was found to increase as the length of the spacer group in the monomer was increased or as the crosslink density in the resin was lowered due to the reduced glass transition temperature which allowed greater mobility and, hence, higher cure. Increasing the curing temperature also resulted in a higher degree of conversion as the network was able to polymerize further before vitrification occurred. For the partially photocured samples, the glass transition temperature was raised as the degree of conversion was increased. Most of the measures of the breadth of the glass transition were found to increase with increased conversion for dimethacrylates with short or stiff backbones (TETDMA and bisGMA) while the transition breadth was independent of conversion for either a more flexible dimethacrylate (NEGDMA) or a dimethacrylate network with a lower crosslink density (50 wt % bisGMA/50 wt % PGEMA). This conclusion was generally confirmed by analysis of the viscoelastic parameters in the frequency domain. It is not clear whether these behaviors resulted from differences in the range of molecular motions available in tight networks or if they were due to spatially heterogeneous regions in the network.
 J Appl Polym Sci 90: 3753–3766, 2003

Key words: photopolymerization; viscoelastic properties; glass transition

INTRODUCTION

Dynamic mechanical thermal analysis (DMTA) has proven to be a valuable tool for studying the network structure of crosslinked polymers.[1–9] A typical DMTA experiment involves measuring the moduli and damping behavior of a material at a given frequency during a temperature ramp up to and beyond the glass transition temperature (T_g) of the material under study. It is commonly observed that highly crosslinked polymers exhibit broad glass transition regions[4,6,9–18] and this can be interpreted as a range of molecular environments in which a variety of chain units are found.[19] Some workers consider that the broadening of the glass transition is representative of a heterogeneous network structure with spatially separated regions having differing relaxation times,[4,6,12,17] while others regard the broad transition to be a natural consequence of the high crosslink density in a homogeneous material with a variety of molecular motions with differing relaxation times.[11,12,20–22]

The effect of the crosslink density on the glass transition can be investigated by studies of a series of polymers with varying concentrations of a crosslinker,[4,23–25] but this alters the chemical composition of the network and so makes comparisons difficult. Alternatively, networks with varying crosslink density can be prepared from mixtures of monomers with varying functionality,[2,13,22,26,27] so that compositional variations are minimized. The effect of crosslinking on the transition also may be studied as a function of conversion; however, this method can present a problem for partially cured materials due the recommencement of polymerization during the DMTA experiment which can increase the T_g and apparently broaden the transition region.[28–31]

During the cure of a thermosetting polymer, the chain extension and formation of crosslinks reduces the mobility of the molecular segments and increases the T_g.[22,27,29,32,33] If the T_g of the material exceeds the curing temperature during the cure process, the material will vitrify,[22,27,29,31,34] freezing in the reactive sites and preventing further reaction. If the sample is then cooled to lower temperatures and is subsequently temperature-ramped in a DMTA experiment, the material will initially be in the glassy state and therefore not capable of reacting until the scanning temperature is in the vicinity of the glass transition temperature of the partially cured resin. As the temperature is increased further, the molecular segments will become more mobile, allowing the reactive sites to recommence polymerization[27,29–31,34]

Correspondence to: W. D. Cook (wayne.cook@spme.monash.edu.au).

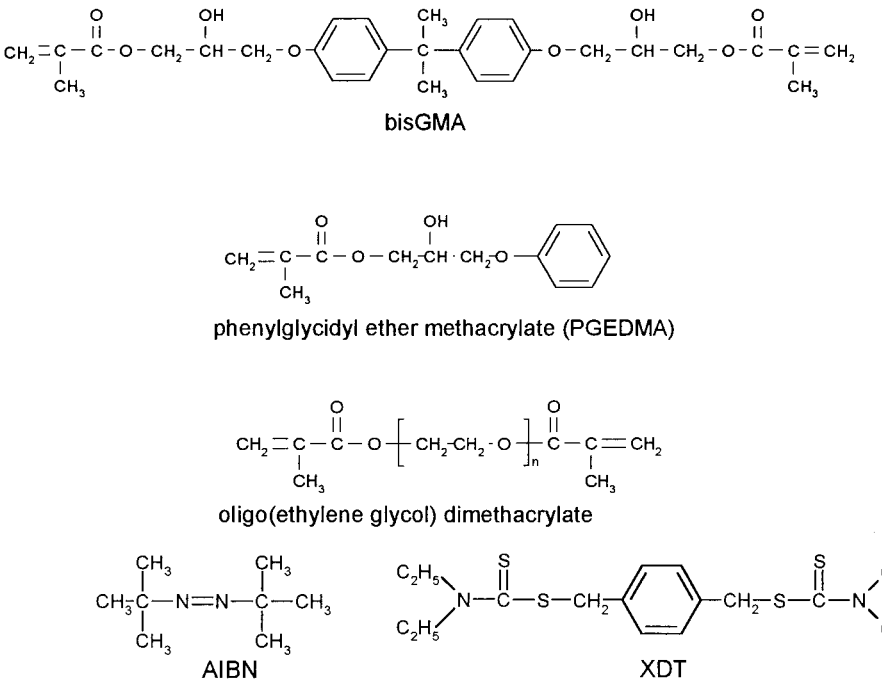

Figure 1 Structures of the monomers: bisGMA, PGEMA, EGDMA (n = 1), DEGDMA (n = 2), TETDMA (n = 4), and NEGDMA (n = 9) and of the initiators.

and this process significantly affects the resultant DMTA spectrum.[29–31]

Recently Kannurpatti et al.[5] used photopolymerization to investigate the thermomechanical properties of partially cured thermosetting polymers using two different classes of photoinitiators. The first type was a conventional photoinitiator that produces radicals which can be trapped in a vitrifying matrix but which are mobilized when the temperature is increased above the T_g. This type of initiator causes complications in the interpretation of the DMTA behavior of partly cured networks because the network structure continues to develop during the thermal analysis experiment.[5] The second initiator type was a photoiniferter which acts as a radical initiator and a chain terminator.[35,36] During irradiation, the photoiniferter produces a carbon-centered radical and a sulfur-centered dithiocarbamyl radical, but only the former can initiate polymerization.[35,36] When the irradiation is terminated, the propagating radical is capped by one of the mobile dithiocarbamyl radical fragments, forming a thermally stable species.[37] Thus, the use of photoiniferters conveniently allows for the examination of the network properties without inadvertently postcuring the sample when it is heated above its T_g. The effectiveness of the photoiniferter technique versus a conventional photoinitiator for thermal analysis of partly cured dimethacrylates was graphically illustrated by Kannurpatti et al.[5]—the DMTA spectrum of the partly photocured network using the conventional initiator exhibited two transitions due to recommencement of curing at elevated temperatures; however, the photoiniferter system had only one transition.

The present study investigated the kinetics of polymerization of dimethacrylate oligomers and evaluated the dynamic mechanical properties after curing to various degrees with a photoiniferter. Dimethacrylates with various structures and flexibility were used to investigate the effect of the molecular structure on the breadth of the transition region.

EXPERIMENTAL

Ethylene glycol dimethacrylate (EGDMA, Fluka, Seelze, Germany), diethylene glycol dimethacrylate (DEGDMA, Mitsubishi, New York, NY), tetraethylene glycol dimethacrylate (TETDMA, Sartomer, West Chester, PA), and nonaethylene glycol dimethacrylate (NEGDMA, Nippon Oil and Fats, Osaka, Japan) were used for kinetic studies of their thermal cure. Bisphenol-A diglycidyl ether dimethacrylate (bisGMA, Esschem, Linwood, PA) and its monomeric analog, phenyl glycidyl ether methacrylate (PGEMA[38]), were additionally used for photocure kinetic studies. The effect of the crosslink density and cure level on the dynamic mechanical behavior of TETDMA, NEGDMA, bisGMA, and a 50/50 w/w copolymer of bisGMA and PGEMA was examined. All monomers were used as received and their structures are presented in Figure 1. The monomers were assumed to have the idealized structures shown in Figure 1 to determine the concentration of the divinyl monomer in the resin and the crosslink densities of the cured networks.

Azobisisobutyronitrile (AIBN, supplied under the trade name Vazo 64 by DuPont, Wilmington, DE) was

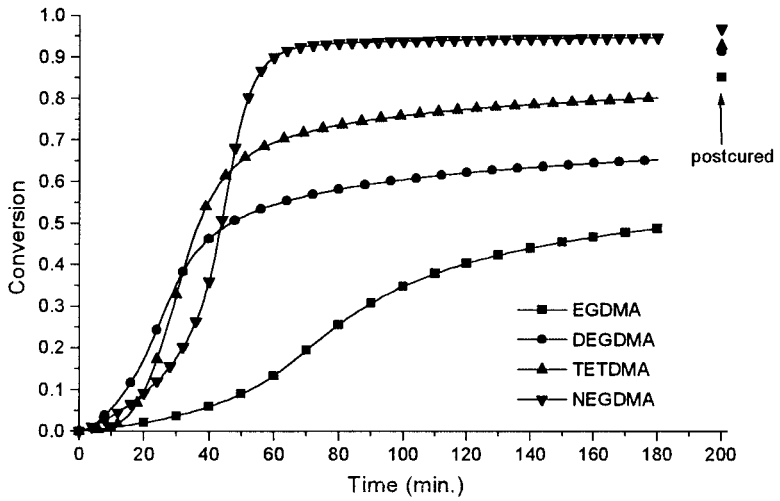

Figure 2 Conversion of dimethacrylates initiated with 0.5 wt % AIBN at 60°C. The curves were moved along the abscissa to remove the induction times of 34, 21, 59, and 17 min for EGDMA, DEGDMA, TETDMA, and NEGDMA. The final conversions as indicated were determined after postcuring at 160°C for 2 h. Only one in 10 datum points is plotted for clarity.

employed as the thermal initiator at 0.5 wt %. *p*-Xylylene bis-(*N*,*N*-diethyldithiocarbamate) (XDT) was employed as the photoiniferter and was synthesized according to the following method[39]: α,α'-dibromo-*p*-xylene was added to an ethanolic solution of sodium diethyldithiocarbamate trihydrate and stirred overnight at room temperature. The suspension was filtered and the precipitated XDT was recrystallized from methanol to give a white solid which was characterized by a melting point [(81–82°C, cf. reference 83–84°C (ref. 39)] and ^{1}H-NMR spectra in $CDCl_3$ (δ = 7.33, s, 4*H*, phenyl; δ = 4.52, s, 4H, SCH_2; δ = 3.88, m, 8H, NCH_2; δ = 1.28, m, 12H, CH_2CH_3). XDT was used at a level of 0.1 wt % in the oligo(ethylene glycol)dimethacrylate monomers and of 0.2 wt % for the cure of bisGMA and for a 50:50 bisGMA/PGEMA blend. Structures for the initiators used are presented in Figure 1.

The ultraviolet-visible spectra of XDT (obtained as an ethanolic solution) and of the oligoethylene oxide-based dimethacrylate monomers (obtained neat) were measured with a Varian Cary 100BIO UV-vis spectrophotometer scanning from 800 to 200 nm using quartz cuvettes with a 10-mm path length. Although the absorbance of the EGDMA, TETDMA, bisGMA, and PGEMA monomers were low (<0.15 cm^{-1} at 365 nm), DEGDMA had an absorbance of 0.4 cm^{-1} at 365 nm, probably due to the presence of an impurity. The absorption coefficient of XDT as measured was 1.5 cm^{-1}(weight percent)$^{-1}$ (equivalent to a molar absorptivity of 60 $M^{-1}cm^{-1}$) at 365 nm.

To evaluate the relative reactivity of the resins, isothermal curing studies were undertaken at 60°C with 0.5 wt % AIBN as an initiator using a Perkin–Elmer Spectrum GX FTIR spectrophotometer with a 2-cm^{-1} resolution. The formulated resin was injected between two glass slides separated by a 1.5-mm-thick silicone gasket and the assembly was placed in a Graseby Specac temperature-controlled cell. Near-infrared (NIR) spectra were taken at the start of the experiment and continuously during the curing progress and the conversion was determined from the change in the absorption intensity of the methacrylate band[40] at 6166 cm^{-1}. The isothermal photopolymerization kinetics were also studied by NIR using the XDT initiator at 20, 60, and 100°C. The samples were cured by irradiating with a Spectroline SB-100PC/FA ultraviolet lamp (Spectronics, Westbury, NY) for various time intervals in a temperature-controlled chamber. The irradiation intensity at the surface of the specimen, measured using an International Light IL1700 radiometer (Newburyport, MA) fitted with a SED033/UVA/W detector, was 4.2 mW/cm^2 at 365 nm. Since the attenuation of the 365-nm radiation was calculated to be 13% for 2-mm-thick 0.2 wt % XDT samples (based on the absorption spectrum of XDT), the samples were alternately photoirradiated on either side to ensure an even cure.

Rectangular specimens were prepared for DMTA in a similar manner as for NIR and their dynamic mechanical properties were measured in a dual cantilever mode using a Rheometric Scientific DMTA IV (Piscataway, NJ) scanning at 2°C/min and with a frequency of either 1 Hz or by a frequency scan ranging from 0.1 to 30 Hz. The glass transition temperature was taken as the temperature at the peak in the tan δ curve at 1 Hz. The Rheometric Orchestrator software V6.5.7 was used to perform time–temperature superposition of the multifrequency data—for these analyses, the T_g was selected as the reference temperature and the time–temperature shift factors were based on an optimization of the superposition of the temperature-normalized real-modulus data.

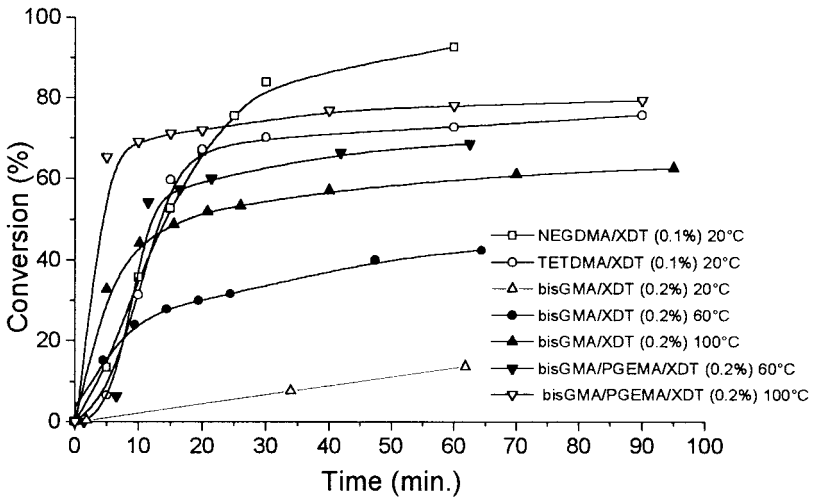

Figure 3 Isothermal conversion of photocured networks as a function of time at various temperatures. The curve for bisGMA/XDT (20°C) was moved along the abscissa to remove the induction time (15 min).

RESULTS AND DISCUSSION

Figure 2 shows the polymerization kinetics of the oligo(ethylene oxide)dimethacrylate resins isothermally cured at 60°C using AIBN as a thermal initiator. All resins exhibited an induction time (not shown in Fig. 2) ranging from 17 to 59 min before the onset of polymerization. The duration of this induction time is probably dependent on the variable amounts of the residual inhibitor in each resin. After the polymerization commences, the rate rapidly increases and then decreases—for EGDMA, DEGDMA, and TETDMA, full cure was not attained at the 60°C curing temperature. Based on the decomposition rate of AIBN[41] in benzene at 60°C, even at the end of the experiment (240 min), more than 74% of the initiator remained, indicating that the incomplete cure was not due to dead-end polymerization.[42] Figure 2 shows that the maximum conversion at 60°C increases as the chain length of the monomer increases and, hence, as the network becomes more flexible, in the order EGDMA < DEGDMA < TETDMA < NEGDMA. The final conversion depends on the structure of the monomers and the mobility of the developing network because, as the reaction proceeds, the T_g increases, and if it approaches the curing temperature, vitrification occurs and polymerization ceases.[27,29,31,43] The cure of NEGDMA is close to complete at 60°C because its flexible backbone results in a T_g for the "fully" cured material which is less than the cure temperature,[43] whereas the T_g of EGDMA increases above the curing temperature.[44] However, after postcuring at 160°C, the conversions of all the systems were increased considerably.

The photopolymerization kinetics of some of the monomers are shown in Figure 3. As found for the thermal cure (Fig. 2), NEGDMA is photocured to a greater extent than is TETDMA because NEGDMA has a more flexible backbone and lower crosslink density, which results in a lower T_g than for TETDMA. A similar effect was found for the aromatic-based methacrylates, bisGMA, and the 50/50 bisGMA/PGEMA blend. PGEMA is a monomethacrylate and so the polymerization results in a linear polymer with no topological restrictions and with an ultimate T_g of approximately 45°C.[45] In contrast, bisGMA is a dimethacrylate which forms a highly crosslinked and rigid structure with a T_g of approximately 180°C.[45] Thus, the final conversion of bisGMA is less than that for the 50/50 bisGMA/PGEMA blend—when cured at the same temperature, the blend cured to a greater conversion because the presence of PGEMA reduces the crosslink density and, hence, the T_g. The effect of temperature on the cure rate and final conversion is also shown in Figure 3—as the cure temperature increases, the rate of propagation increases and vitrification occurs at a later stage in the polymerization process so that a higher conversion is attained.

DMTA was performed on samples that had been partially photocured and the T_g determined from the maximum in tan δ. Figure 4 illustrates the variation in T_g as a function of conversion for the long- and flexible-chain dimethacrylate, NEGDMA, for the short- but flexible-chain dimethacrylate, TETDMA, for the long- but rigid-chain dimethacrylate, bisGMA, and for the rigid but less highly crosslinked bisGMA/PGEMA. For the same level of conversion, bisGMA exhibits the highest T_g due to the high rigidity provided by the bisphenol-A backbone, whereas NEGDMA has the lowest T_g because it has a very flexible backbone and because the network has as low crosslink density. With increasing levels of photocuring, T_g increases due to the reduction in the concentration of a plasticizing monomer and because the developing network structure restricts the molecular motion.[12,13,27,31,46] In agreement with that found by other

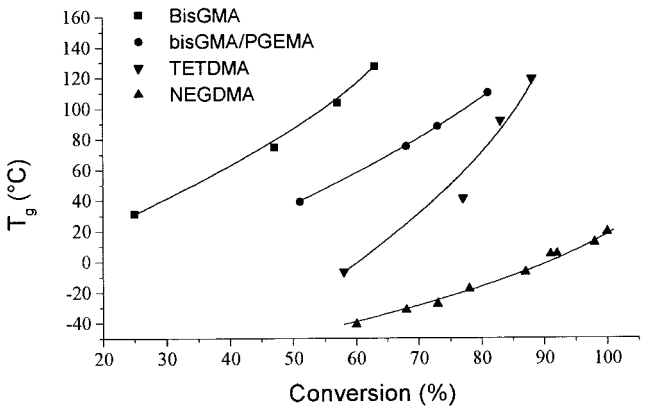

Figure 4 T_g of photocured dimethacrylates as a function of degree of conversion.

workers,[12,27,31,32,46] the dependence of T_g on the conversion tends to increase as the degree of crosslinking increases.

The effect of conversion on the dynamic properties of photocured networks formed from NEGDMA, bisGMA/PGEMA, bisGMA, and TETDMA is shown in Figures 5–8. In each case, the tan δ passes through a maximum and the real modulus undergoes a large reduction associated with the glass transition. None of the DMTA traces show the double-peaked behavior typically observed in undercured resins,[30,31] because the propagating radicals formed during photoinitiation are capped by the dithiocarbamate radicals when the irradiation ceases.[35,36] As noted above, an increase in the crosslink density results in an increase in T_g. As expected from the theory of rubber elasticity,[47] the modulus in the rubber region also increases with increasing conversion due to the higher crosslink density and thus greater concentration of elastically active strands. After attaining the rubbery region, the modulus remains relatively constant, which is also confirmation that the partially cured networks are thermally

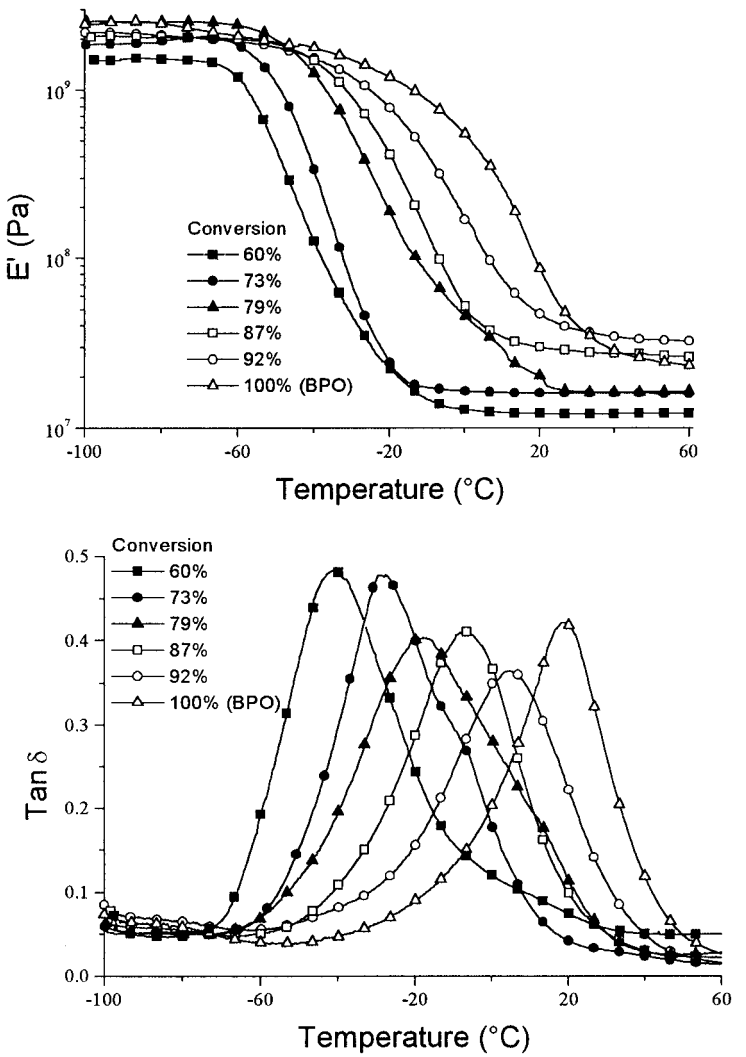

Figure 5 Storage modulus (E') and tan δ curves (at 1 Hz) for NEGDMA photocured with XDT at 20°C for varying times and postcured at 70°C for 30 min, resulting in the conversions indicated. For a comparison, the DMTA behavior is shown for a thermally cured sample using AIBN as an initiator. Only one in 20 of the datum points is shown to aid clarity.

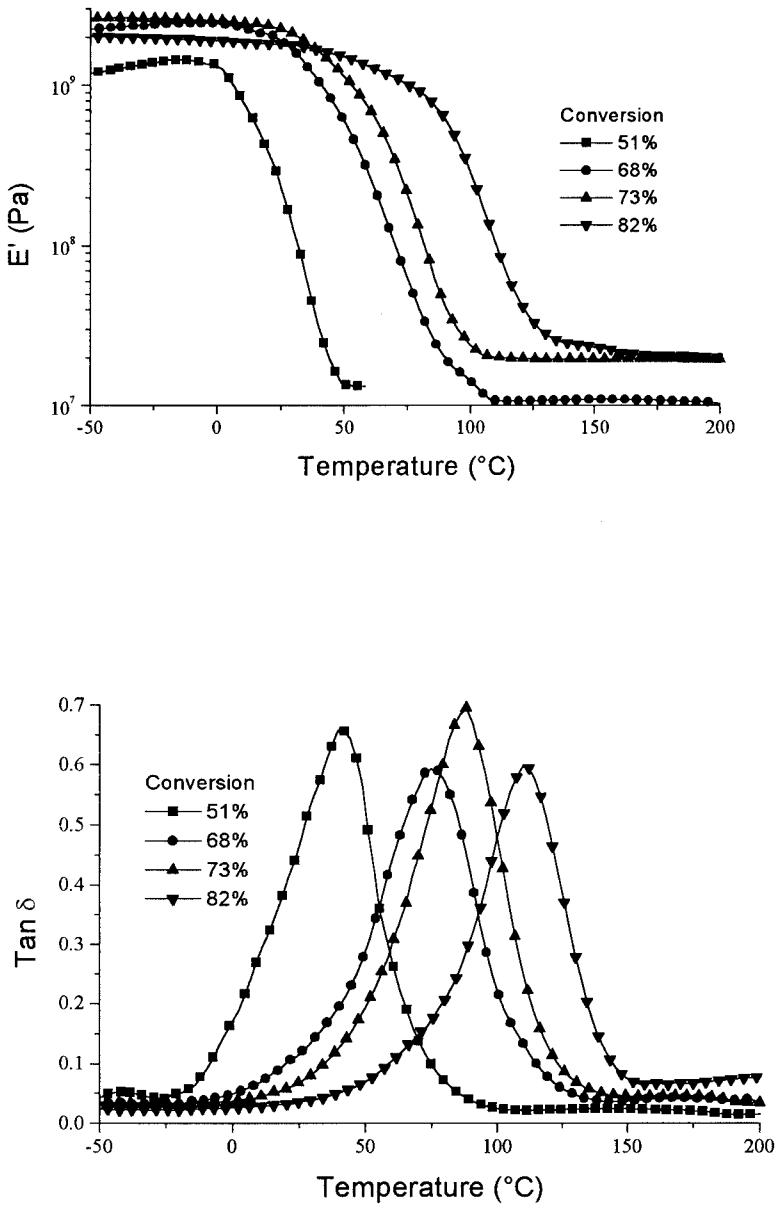

Figure 6 E' and tan δ curves (at 1 Hz) for 50 wt % bisGMA/50 wt % PGEMA cured to various conversions. Only one in two of the data points is shown to aid clarity.

stable. A comparison of the rubbery moduli of the polymers reveals that, for the same level of conversion, the modulus varies in the order

$$\text{bisGMA} > \text{TETDMA} > \text{NEGDMA} \geq \text{bisGMA/PGEMA}$$

This ranking is not the same as the crosslink densities, which (for the same level of cure) is

$$\text{TETDMA} > \text{bisGMA} > \text{NEGDMA} > \text{bisGMA/PGEMA}$$

and this difference is probably due to the non-Gaussian chain statistics[48] of these highly crosslinked materials—of all the materials, the chains in bisGMA are the most rigid and this appears to increase the moduli of bisGMA-containing networks higher than they would otherwise be.

Figures 5 and 6 suggest that the transition breadth, as measured by the real-modulus and tan δ curves, for NEGDMA and for the 50:50 bisGMA/PGEMA copolymer is virtually independent of conversion; however, for the TETDMA and bisGMA samples (Figs. 7 and 8), the breadth appears to increase with higher cure levels. Plots of normalized tan δ versus the departure from T_g ($T - T_g$; not shown) revealed that the breadth of the tan δ curve for the partly cured NEGDMA and bisGMA/PGEMA systems was essentially independent of the degree of conversion for each system,

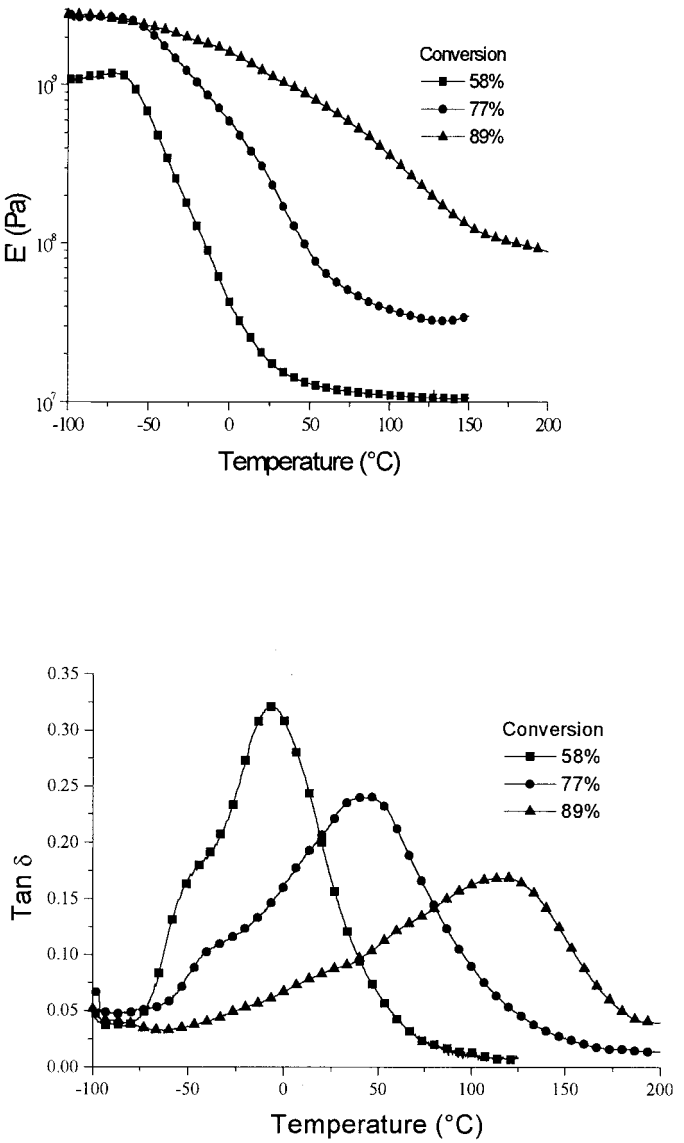

Figure 7 E' and tan δ curves (at 1 Hz) for TETDMA photocured to various conversions using XDT. Only one in 20 of the data points is shown to aid clarity.

while the breadth of tan δ increases with the degree of cure for TETDMA (due to a broadening on the low-temperature side) and for bisGMA (due to symmetric broadening). The breadth of the tan δ curve, expressed as the full width at half-height in Table I, confirms the conclusion that the tan δ breadth does not necessarily increase with increased cure. In addition, a comparison of the breadths of the four resin systems listed in Table I does not exhibit a systematic dependence on the crosslink density but shows that the less mobile structures (TETDMA with a short flexible chain or bisGMA with long rigid chains) tend to have broader transitions.

Both the real (E') and loss moduli (E'') can be expressed in terms of the various relaxational modes involved in the transition via the distribution of relaxation times.[49] The tan δ is defined as the ratio of E''/E' and so has a more complex relationship to the distribution of molecular relaxation times. Thus, it might be argued that the breadth of the glass transition should be determined from the loss modulus rather than from tan δ. Table I lists these values. Interestingly, the breadth of the loss modulus does not show a systematic dependence on the monomer structure, but, in contrast to the real-modulus and tan δ data, as the cure advances, a broadening is found in the E'' curves of all the networks (with the possible exception of the bisGMA/PGEMA system). These data must be treated with caution as they are less reliable than are the tan δ data, since they are not directly determined experimentally but are calculated from the tan δ and the real modulus. In addition, E'' is more sensitive to overlap of the sub-T_g relaxations with the glass transition since the low-temperature (high stiffness) side of the glass transition is more accentuated in the E'' curve compared with the tan δ curve.

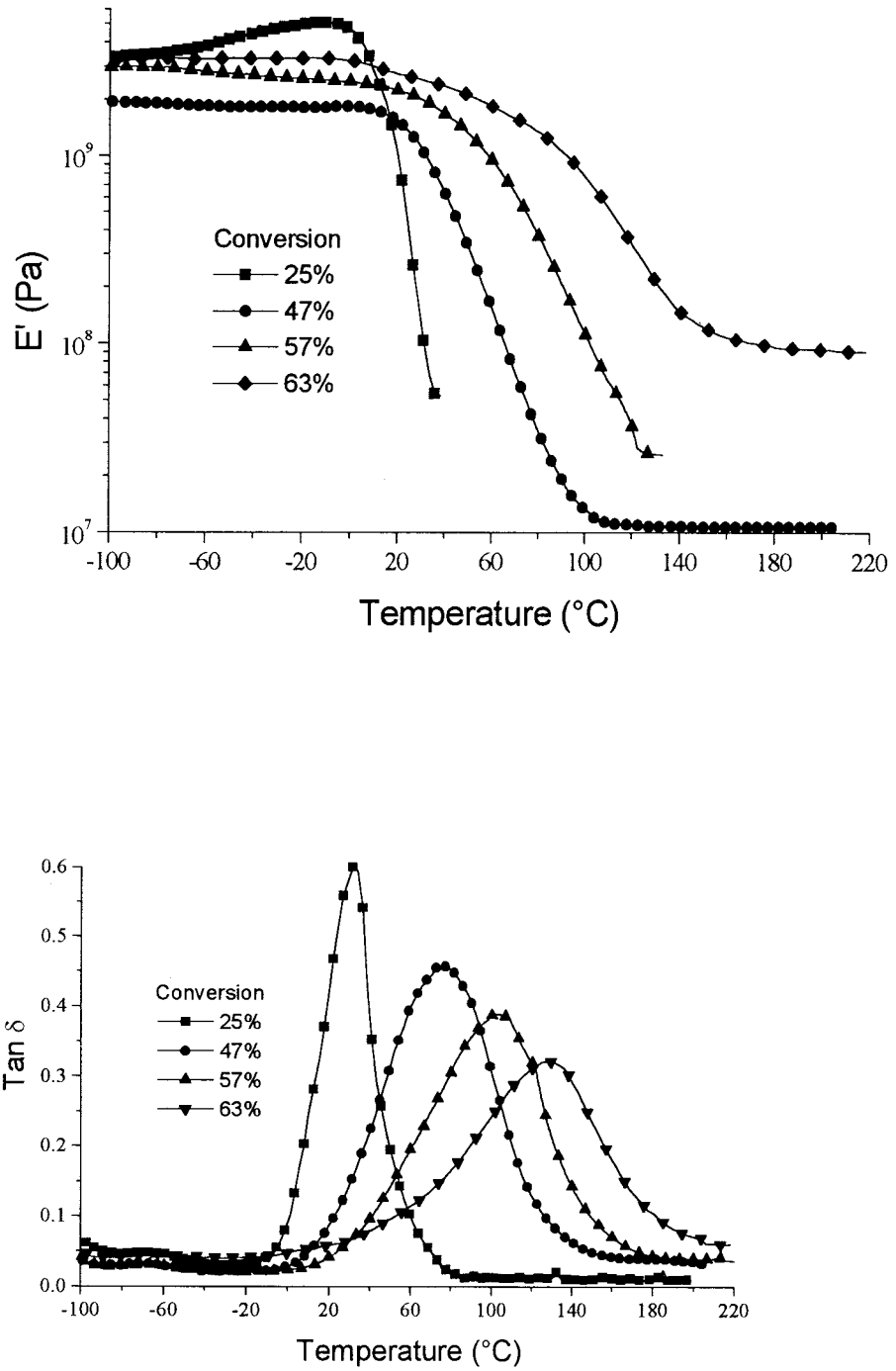

Figure 8 E' and tan δ curves (at 1 Hz) for bisGMA cured to various conversions using XDT. Only some of the points are shown to aid clarity.

By analogy with the loss modulus, the loss compliance [D'' given by the formula[49] $E''/(E'^2 + E''^2)$] can also be expressed in terms of the range of molecular motions by the distribution of retardation times.[49] Contrary to the trends shown by E'', but in agreement with the tan δ and E' data, the loss compliance data suggest that the breadth of the bisGMA/PGEMA and NEGDMA transitions show no systematic dependence on conversion, whereas the bisGMA and TETDMA networks do tend to shown an increase in breadth.

It is not clear whether the variations in the transition breadth are inherently due to crosslinking or if they are due to heterogeneity in the crosslinked structure. As discussed above, the bisGMA/PGEMA networks have the lowest crosslink density (see Table I), the NEGDMA and bisGMA networks have intermediate crosslink density, and the TETDMA networks have the highest crosslink density. This trend partly agrees with the E', tan δ, and D'' transition breadths, since the bisGMA/PGEMA and NEGDMA have narrow transi-

TABLE I
Variation of the Full width of the tan δ and *G″* Curves at Half-height (fwhh) with Conversion for NEGDMA, TETDMA, bisGMA, and 50/50 bisGMA/PGEMA Copolymer

Dimethacrylate system	Concentration of divinyl monomers (mol/g)	Conversion (%)	Crosslink density[a] (mol/g)	fwhh (°C) from tan δ	fwhh (°C) from *E″*	fwhh (°C) from *D″*
50/50 bisGMA/PGEMA	9.75×10^{-4}	51	4.97×10^{-4}	42	36	24
	9.75×10^{-4}	68	6.63×10^{-4}	45	64	37
	9.75×10^{-4}	73	7.12×10^{-4}	42	67	29
	9.75×10^{-4}	82	7.99×10^{-4}	41	59	29
bisGMA	1.95×10^{-3}	25	4.88×10^{-4}	29	24	18
	1.95×10^{-3}	47	9.18×10^{-4}	67	46	43
	1.95×10^{-3}	57	1.11×10^{-3}	72	63	34
	1.95×10^{-3}	63	1.23×10^{-3}	86	ca. 110[b]	65
NEGDMA	1.81×10^{-3}	60	1.09×10^{-3}	38	23	58
	1.81×10^{-3}	69	1.25×10^{-3}	36	26	33
	1.81×10^{-3}	73	1.32×10^{-3}	39	31	24
	1.81×10^{-3}	79	1.43×10^{-3}	48	45	40
	1.81×10^{-3}	87	1.57×10^{-3}	38	50	26
	1.81×10^{-3}	92	1.67×10^{-3}	40	ca. 78[b]	22
	1.81×10^{-3}	100	1.81×10^{-3}	32	ca. 70[b]	18
TETDMA	3.03×10^{-3}	58	1.75×10^{-3}	76	35	59
		77	2.33×10^{-3}	109	ca. 75[b]	82
		89	2.70×10^{-3}	137	ca. 200[b]	84

[a] Defined here as the concentration of divinyl molecules connected to the network estimated from the product of the concentration of divinyl molecules in the resin times the fractional conversion.
[b] Due to the high loss modulus values on the low-temperature side of the transition and overlap with other low-temperature relaxations, these values are only approximate.

tions which do not appear to change with curing, whereas the bisGMA and TETDMA have the broadest transitions which increase in breadth with higher levels of curing. Alternatively, Kannurpatti et al. suggested[5,6,50] that the broad tan δ curves imply a wider distribution of relaxation times due to a more spatially heterogeneous polymer, which depends strongly on the crosslinking density of the system and the nature of the crosslinking monomers. According to Bowman et al.,[6,51] longer-chain dimethacrylates (such as NEGDMA) or longer-chain and more rigid dimethacrylates (such as bisGMA) are less likely to form the cycles which lead to microgels and heterogeneity. However, this argument does not agree with the data since NEGDMA has one of the narrowest transitions while bisGMA has one of the widest. It is noteworthy that, unlike TETDMA, NEGDMA is not a pure monomer but also contains shorter and longer oligo(ethylene oxide)dimethacrylates,[44] but this heterogeneity in the crosslink density does not result in a broad transition region.

As noted by McCrum et al.[19] the breadth of the viscoelastic properties as a function of temperature is not only dependent on the distribution of relaxation times but is also dependent on the activation energies of the molecular motions in the transition. In an attempt to remove this additional factor in the transition breadth, frequency scans were undertaken during some of the DMTA experiments. These data were analyzed by time–temperature superposition of the real-modulus data and the resulting shift factors were applied to the other viscoelastic parameters. Figures 9–14 show the superposed data for the systems studied. The superposition seems reasonable for the NEGDMA resin but is not so good for the other resins. In part, this may be due to the breadth of the transition and the narrow range of frequencies studied, because broad curves are more difficult to accurately superimpose. In addition, the errors may be due to the overlap of other relaxations with the glass transition region because the time–temperature superposition principle assumes[19] that, when the temperature is increased, all relaxation times are decreased by same amount—that is, the shift factor (and, thus, the effective activation energy at each temperature) is the same for all the molecular motions occurring in the transition.[19] The temperature dependence of the shift factors (a_T), over the temperature range of approximately −50° below the T_g to 100° above the T_g, were analyzed in terms of the WLF equation:

$$\log(a_T) = \log\left(\frac{\omega_{\text{ref}}}{\omega}\right) = \frac{-c_1(T - T_{\text{ref}})}{c_2 + T - T_{\text{ref}}}$$

where T and ω are the measurement temperatures and frequencies and T_{ref} is the reference temperature where the tan δ exhibits a peak at a frequency, ω_{ref}, of 1 Hz. The values for c_1 and c_2 are listed in Table II, as are the statistical R-squared parameter. Since the fits of the WLF equation to the shift factors were not very good (as indicated by the low R-squared values), the values of c_1 and c_2 are likely to be only approximate.

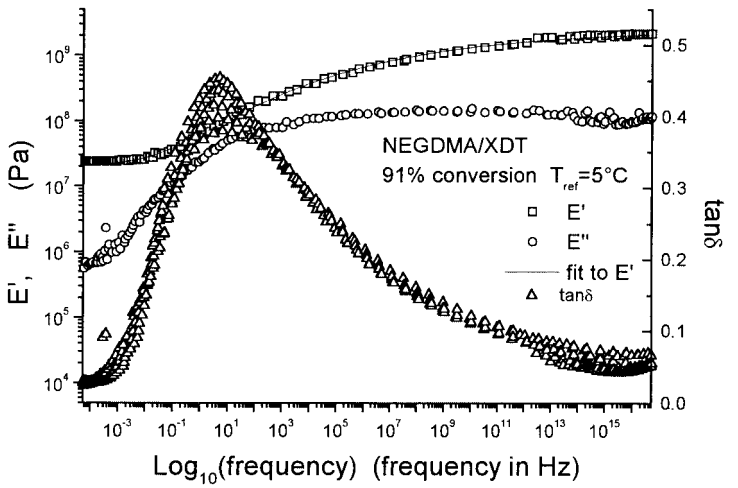

Figure 9 E', E'', and tan δ versus frequency for NEGDMA using time–temperature superposition of the real-modulus data. The samples were cured to 91% conversion, by photocuring with XDT as an initiator at 20°C for 60 min followed by postcuring at 70°C for 30 min. The reference temperature of 5°C is the temperature at which the tan δ passed through a maximum at 1 Hz. To increase clarity, not all points are plotted. The solid line shows the fit to the E' data using the stretched exponential.

The "universal values" for c_1 and c_2 should be 16 and 50°C if the temperature at the tan δ peak is accepted to be the glass transition temperature.[49] Table II shows that the value of c_1 is close to the universal value. According to the free-volume derivation of the WLF equation,[49] c_1 is related to the free volume at the T_g and so it appears that this is not significantly affected by crosslinking. In contrast, c_2 is much larger than is the theoretical value and this may be a consequence of the high crosslink densities in these networks, since, in the free-volume derivation, c_2 is given by the free volume at the T_g divided by the free-volume expansion coefficient[49] and it is known that the latter decreases with increased crosslink density.[21] The WLF parameters, c_1 and c_2, were also weakly correlated with themselves (with an r-squared value of 0.38) and with the T_g (with an r-squared values of 0.30 and 0.59, respectively), although there does not appear to be a theoretical justification for this observation.

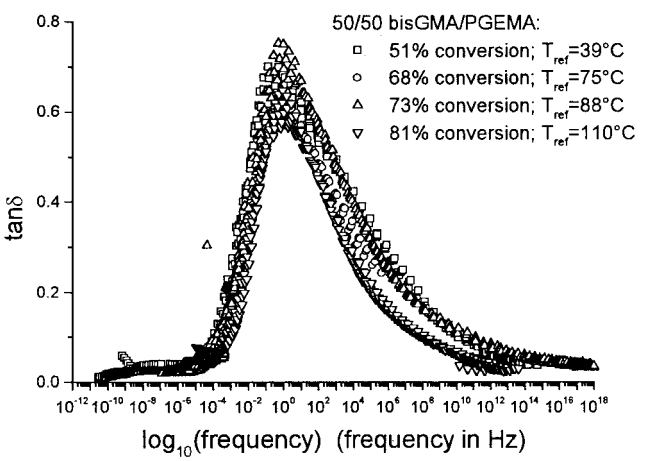

Figure 10 Tan δ versus frequency for 50/50 bisGMA/PGEMA using time–temperature superposition of the real-modulus data. The samples were cured to the conversions, as shown, by photocuring for different times at 60°C (or 100°C for the sample with 81% conversion) with XDT as an initiator. The reference temperature for each sample was the temperature at which the tan δ passed through a maximum at 1 Hz. To increase clarity, not all points are plotted.

Figures 9–14 show that the transition region of the partly cured networks is very broad and spans many decades, as was observed by Kannurpatti et al.[5,6,50] for other dimethacrylate networks. Table II lists the full widths at half-height for the frequency dispersion of tan δ, E'', and D''. It is noteworthy that, for a particular network, the widths of these functions are quite dissimilar, with E'' giving the broadest transition, and D'', the narrowest. The frequency dispersion of the tan δ curves are narrowest for bisGMA/PGEMA and NEGDMA and widest for bisGMA and TETDMA, as was observed for the temperature dependence. A similar correlation was observed for the dynamic loss compliance but the loss modulus data did not show a clear trend. Contrary to that found for the temperature-dependent data, for each particular dimethacrylate, there was no clear trend with conversion, but this may be a result of the limited experimental data.

Another measure of the range of relaxation times was obtained by fitting the superposed real-modulus (E') data to the stretched exponential expression:

$$E' = E_0 e^{-(1/\omega\tau)^n} + E_\infty$$

where E_0 and E_∞ are the unrelaxed (glassy) and relaxed (rubbery) moduli, respectively; ω, the frequency; τ, the relaxation time; and the exponent n, the distribution parameter. This equation was adapted from the

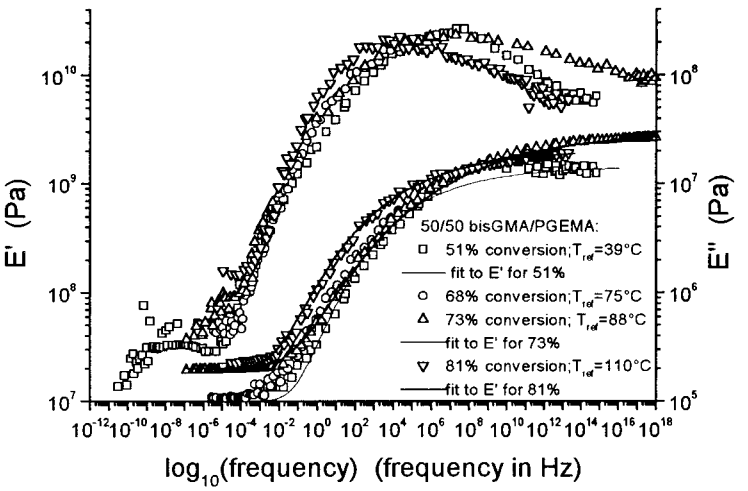

Figure 11 E' and E'' versus frequency for 50/50 bisGMA/PGEMA using time–temperature superposition of the real-modulus data. The samples were cured to the conversions, as shown, by photocuring for differing times at 60°C (or 100°C for the sample with 81% conversion) with XDT as an initiator. The reference temperature for each sample was the temperature at which the tan δ passed through a maximum at 1 Hz. To increase clarity, not all points are plotted. The solid lines show the fit to the E' data for the sample having 51, 73, and 81% conversion, using the stretched exponential.

Williams–Watts equation[52] for the stress-relaxation modulus on the basis that $E(t) \approx E'(\omega)$ at $\omega = 1/t$. This approximation was also used by Kannurpatti et al.[5] and is valid provided that the distribution of relaxation times is broad.[53] In fact, the glass transition region in dimethacrylate networks is very broad compared with that in networks formed by step-growth polymerization[54] or linear polymers.[55] The fit of the data to the stretched exponential, shown in Figures 9, 11, 13, and 14, is good for NEGDMA and bisGMA/PGEMA but is poorer for bisGMA and TETDMA. The values of the distribution parameter are listed in Table II. In contrast to that found with linear polymers,[53] where the distribution parameter is often close to 0.5, Table I shows that n ranges from 0.05 to 0.12, suggesting a wide range of relaxation times. These results are similar to those obtained by Kannurpatti et al.[5,6] using DMTA methodology and those obtained by Young et al.[56] by dielectric studies of related methacrylate networks. Although the distribution parameter tended to be smaller for the TETDMA and bisGMA networks, no clear correlation with the structure, crosslink density, or transition breadth was obvious.

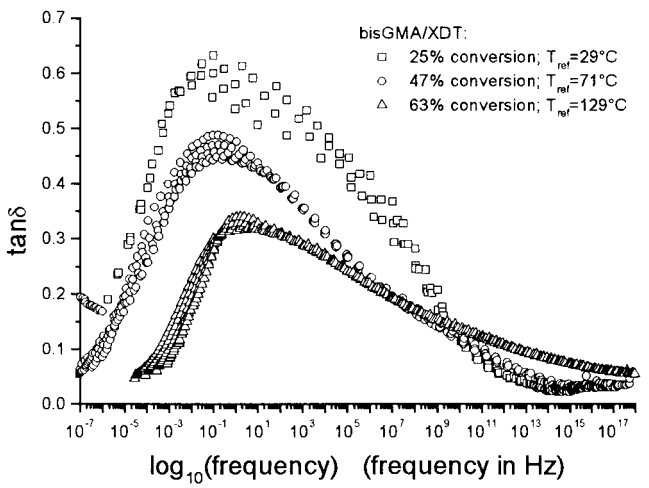

Figure 12 Tan δ versus frequency for bisGMA using time–temperature superposition of the real-modulus data. The samples were cured to the conversions, as shown, by photocuring for differing times at 60°C (or 150°C for the sample with 63% conversion) with XDT as an initiator. The reference temperature for each sample was the temperature at which the tan δ passed through a maximum at 1 Hz. To increase clarity, not all points are plotted.

CONCLUSIONS

The isothermal thermal polymerization kinetics of a series of dimethacrylate oligomer resins was studied and compared with the photopolymerization kinetics using an iniferter radical polymerization mechanism. The final isothermal conversion increased as the flexibility of the polymer backbone increased and was also increased by higher curing temperatures—as the monomer flexibility or the curing temperature is increased, the network vitrifies at a later stage in the polymerization and results in higher conversion.

An iniferter photoinitiator was used to produce four series of highly crosslinked polymers with varying conversion but no trapped radicals so that the thermomechanical properties of the network polymer could be characterized by DMTA as a function of the degree of conversion without the complicating effect of thermal cure. Characterization of the thermomechanical properties shows that the T_g and the rubbery modulus rises as the degree of conversion and, thus, the crosslink density is increased. The breadth of the transition in the temper-

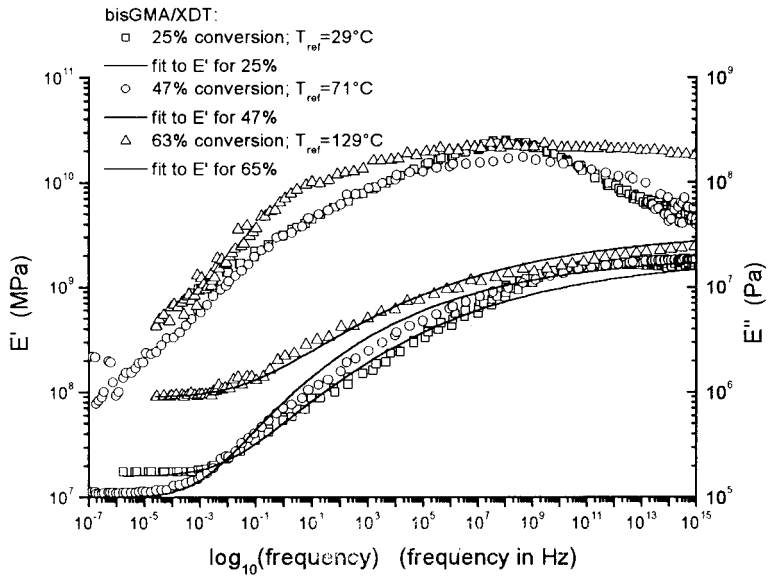

Figure 13 E' and E'' versus frequency for bisGMA using time–temperature superposition of the real-modulus data. The samples were cured to the conversions, as shown, by photocuring for different times at 60°C (or 150°C for the sample with 63% conversion) with XDT as an initiator. The reference temperature for each sample was the temperature at which the tan δ passed through a maximum at 1 Hz. To increase clarity, not all points are plotted. The solid lines show the fit to the E' data using the stretched exponential.

ature domain was relatively independent of the conversion for NEGDMA and bisGMA/PGEMA, as shown by the E', D'', and tan δ data—the E'' data did not follow this trend, but this is believed to be due to an overlap of the transition region with sub-T_g relaxations. The transition breadth of the bisGMA and TETDMA networks did increase with higher conversion and networks formed from these monomers had the broadest glass transition. This may suggest that there is a wider range of molecular motions in networks with less flexible backbones (short chains as in TETDMA or stiff backbones as in bisGMA). Alternatively, these data may suggest that the TETDMA and bisGMA networks are spatially heterogeneous.

Time–temperature superposition was used to derive the viscoelastic parameters as a function of the

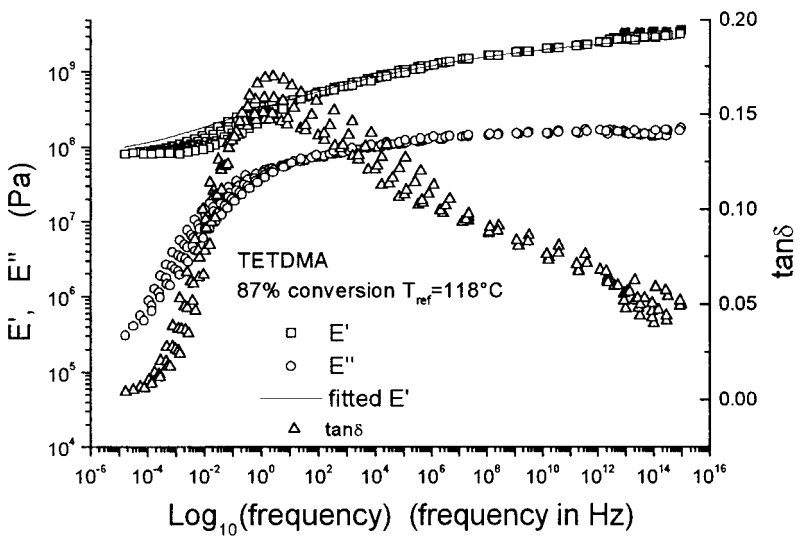

Figure 14 E', E'', and tan δ versus frequency for TETDMA using time–temperature superposition of the real-modulus data. The samples were cured to 89% conversion, by photocuring with XDT as an initiator at 20°C for 90 min followed by postcuring at 70°C for 30 min. The reference temperature of 118°C is the temperature at which the tan δ passed through a maximum at 1 Hz. To increase clarity, not all points are plotted. The solid line shows the fit to the E' data using the stretched exponential.

TABLE II
WLF Parameters and Williams–Watts Distribution Parameter as a Function of Conversion in NEGDMA, TETDMA, bisGMA, and 50:60 bisGMA/PGEMA Copolymer

Resin	Conversion (%)	Crosslink density[a] (mol/g)	fwhh (frequency decades) from tan δ	fwhh (frequency decades) from E''	fwhh (frequency decades) from D''	c_1	c_2 (°C)	r^2	T_{ref} (°C)	n
bisGMA/PGEMA	51	4.98×10^{-4}	6.5	7.6	2.4	16	111	0.94	39	0.133 ± 0.002
bisGMA/PGEMA	68	6.64×10^{-4}	6.2	[b]	2.4	9	67	0.97	75	[c]
bisGMA/PGEMA	73	7.13×10^{-4}	6.2	13.4	3.3	11	110	0.88	88	0.087 ± 0.001
bisGMA/PGEMA	81	7.91×10^{-4}	5.9	8.6	2.6	21	178	0.70	110	0.116 ± 0.002
bisGMA	25	4.88×10^{-4}	11.9	6.7	4.5	11	41	0.93	31	0.074 ± 0.001
bisGMA	47	9.18×10^{-4}	10.1	11.1	4.3	18	121	0.97	75	0.087 ± 0.001
bisGMA	63	1.23×10^{-3}	11.2	>17	4.1	20	225	0.60	129	0.078 ± 0.005
NEGDMA	91	1.65×10^{-3}	7.5	ca. 14.3	2.9	11	87	0.94	5	0.081 ± 0.002
TETDMA	89	2.64×10^{-3}	12.4	[b]	3.8	13	238	0.84	118	0.057 ± 0.001

[a] Defined here as the concentration of divinyl molecules connected to the network estimated from the product of the concentration of divinyl molecules in the resin times the fractional conversion.
[b] Not measurable as no maximum was observed in the superposed E'' data.
[c] Data range not sufficiently wide to fit.

oscillation frequency. The shift factors were reasonably well fitted by the WLF equation, but the WLF constant, c_2, was quite different from the universal value. The transition breadth in the frequency domain generally showed the same trends as in the temperature domain. The E' data were fitted to the stretched exponential, and although the magnitude of the distribution parameter indicated that these materials have broad transitions, they did not shown any clear dependency on network structure or architecture.

The authors would like to thank Prof. Chris Bowman, from the University of Colorado, for providing one of the authors (T. F. S.) the opportunity to work in his laboratory since this stay provided the original motivation for the present study. One of the authors (T. F. S.) is also pleased to acknowledge the support provided by the APA(I) scholarship from the Australian Government and another of the authors (N. I.) gratefully acknowledges the CRC for Polymers for providing her a summer vacation scholarship.

References

1. Tobolsky, A. V.; Katz, D.; Takahashi, M.; Schaffhauser, R. J Polym Sci Part A 1964, 2, 2749.
2. Shibayama, K.; Suzuki, Y. J Polym Sci Part A 1965, 3, 2635.
3. Cook, W.; Delatycki, O. Eur Polym J 1978, 14, 369.
4. Simon, G. P.; Allen, P. E. M.; Williams, D. R. G. Polymer 1991, 32, 2577.
5. Kannurpatti, A. R.; Anderson, K. J.; Anseth, J. W.; Bowman, C. N. J Polym Sci Part B Polym Phys 1997, 35, 2297.
6. Kannurpatti, A. R.; Anseth, J. W.; Bowman, C. N. Polymer 1998, 39, 2507.
7. Lovell, L. G.; Berchtold, K. A.; Elliott, J. E.; Lu, H.; Bowman, C. N. Polym Adv Technol 2001, 12, 335.
8. Lu, H.; Lovell, L. G.; Bowman, C. N. Macromolecules 2001, 34, 8021.
9. Scott, T. F.; Cook, W. D.; Forsythe, J. S. Eur Polym J 2002, 38, 705.
10. Kwei, T. K. J Polym Sci A-2 1966, 4, 943.
11. Shibayama, K.; Suzuki, Y. J Polym Sci Part A 1965, 3, 2637.
12. Nielsen, L. J Macromol Sci-Rev Macromol Chem C 1969, 3, 69.
13. Cook, W. D. Eur Polym J 1978, 14, 715.
14. Kloosterboer, J. G.; Lijten, G. F. M. C. Polymer 1990, 31, 95.
15. Lange, J.; Manson, J.-A. E.; Hult, A. Polymer 1996, 37, 5859.
16. Nabeth, B.; Gerard, J.; Pascault, J. J Appl Polym Sci 1996, 60, 2113.
17. Young, J. S.; Bowman, C. N. Macromolecules 1999, 32, 6073.
18. Mayr, A. E.; Cook, W. D.; Edward, G. H.; Murray, G. J. Polym Int 2000, 49, 293.
19. McCrum, N. G.; Read, B. E.; Williams, G. Anelastic and Dielectric Effects in Solid Polymers; Dover: New York, 1967.
20. Ueberreiter, K.; Kanig, G. J Chem Phys 1950, 18, 399.
21. Mason, P. Polymer 1964, 5, 625.
22. Cao, Z.; Galy, J.; Gerard, J. F.; Sautereau, H. Polym Networks Blends 1993, 4, 15.
23. Andrady, A. L.; Sefcik, M. D. J Polym Sci Polym Phys Ed 1983, 21, 2453.
24. Bellenger, V.; Verdu, J.; Morel, E. J Polym Sci Part B Polym Phys 1987, 25, 1219.
25. Nabeth, B.; Corniglion, I.; Pascault, J. J Polym Sci Part B Polym Phys 1996, 34, 401.
26. Loshaek, S. J Polym Sci 1955, 15, 391.
27. Wise, C. W.; Cook, W. D.; Goodwin, A. A. Polymer 1997, 38, 3251.
28. Babayevsky, P.; Gillham, J. J Appl Polym Sci 1973, 17, 2067.

29. Aronhime, M.; Gillham, J. Adv Polym Sci 1986, 78, 83.
30. Wisanrakkit, G.; Gillham, J. J Appl Polym Sci 1991, 42, 2453.
31. Cook, W. D.; Simon, G. P.; Burchill, P. J.; Lau, M.; Fitch, T. J. J Appl Polym Sci 1997, 64, 769.
32. Pascault, J. P.; Williams, R. J. J. J Polym Sci Part B Polym Phys 1990, 28, 85.
33. Hale, A.; Macosko, C. W.; Bair, H. E. Macromolecules 1991, 24, 2610.
34. Scott, T. F.; Cook, W. D.; Forsythe, J. S. Polymer 2002, 43, 5839.
35. Otsu, T.; Yoshida, M. Makromol Chem Rapid Commun 1982, 3, 127.
36. Kannurpatti, A. R.; Lu, S.; Bunker, G. M.; Bowman, C. N. Macromolecules, 1996, 29, 7310.
37. Moad, G.; Solomon, D. H. The Chemistry of Free Radical Polymerization; Pergamon: Oxford, 1995.
38. Cook, W. D. J Appl Polym Sci 1991, 42, 1259.
39. Otsu, T.; Kuriyama, A. Polym Bull 1984, 11, 135.
40. Rey, L.; Galy, J.; Sautereau, H. Macromolecules 2000, 33, 6780.
41. Hook, J. V.; Tobolsky, A. J Am Chem Soc 1958, 80, 779.
42. O'Driscoll, K. F.; McArdle, S. A. J Polym Sci 1959, 40, 557.
43. Xia, W. Z.; Cook, W. D. Polym Mater Sci Eng 2001, 84, 600.
44. Cook, W. D. J Polym Sci Part A Polym Chem 1993, 31, 1053.
45. Dean, K.; Cook, W. D., unpublished results, 2002.
46. Simon, S.; Gillham, J. J Appl Polym Sci 1993, 47, 461.
47. Flory, P. J. Principles of Polymer Chemistry; Cornell University: Ithaca, NY, 1953.
48. Smith, T. L. J Polym Sci Polym Symp 1974, 46, 97.
49. Ferry, J. D. Viscoelastic Properties of Polymers; Wiley: New York, 1970.
50. Kannurpatti, A. R.; Bowman, C. N. Macromolecules 1998, 31, 3311.
51. Elliot, J. E.; Lovell, L. G.; Bowman, C. N. Dent Mater 2001, 17, 221.
52. Williams, G.; Watts, D. C. Trans Faraday Soc 1971, 67, 1323.
53. Matsuoka, S. Relaxation Phenomena in Polymers; Hanser: Munich, Germany, 1992.
54. Wise, C. W.; Cook, W. D.; Goodwin, A. A. Polymer 2000, 41, 4625.
55. Tobolksy, A. V.; Katz, D.; Takahashi, M.; Schaffhauser, R. J Polym Sci Part A 1964, 2, 2749.
56. Young, J. S.; Kannurpatti, A. R.; Bowman, C. N. Macromol Chem Phys 1998, 199, 1043.